Flow, Turbulence and Combustion **65:** 113–131, 2000.

Mixing in Isotropic Turbulence with Scalar Injection and Applications to Subgrid Modeling

M. ELMO[1], A. MOREAU[1], J.P. BERTOGLIO[1] and V.A. SABEL'NIKOV[2]
[1]*Laboratoire de Mécanique des Fluides et d'Acoustique, UMR 5509, Ecole Centrale de Lyon, 36 Av. Guy de Collongue, 69130 Ecully, France*
[2]*TSAGI, Zhukovsky Moscow Region, 140160, Russia*

Received 14 December 1999; accepted in revised form 15 February 2001

Abstract. A new technique for injecting scalar fluctuations in a DNS of isotropic turbulence is presented. It is used to study statistically steady states associated with different levels of mixing. The results are analysed in terms of spectra and PDF, and they are used as a data base to investigate the effect of the filtering operation that is performed in LES. It is shown that the PDF of the scalar is substantially affected by the filtering operation. It is also shown that the Cook and Riley [1] subgrid model allows reconstruction of a PDF which is in fairly good agreement with the unfiltered DNS results. The consequences of estimating the scalar subgrid variance by scale similarity assumptions are investigated. It is found that the results are improved by a local determination of the model constant.

Key words: mixing, turbulence, probability density function, subgrid-scale model.

1. Introduction

The mixing of a passive scalar by turbulence is of interest for many practical applications. For description of turbulent reacting flows, the knowledge of low order statistical moments is insufficient to account for the non linear nature of the chemical reaction term. Indeed what is needed is an estimation of the probability density function (PDF) of the scalar fluctuations. In particular, in the equilibrium chemistry limit, most quantities of interest, such as the mass fraction of the product or the radiation source term, can be computed from the PDF of a single conserved scalar, called the mixture fraction [2]. It is known that the equation governing the evolution of the PDF is not closed and contains terms such as the conditional scalar dissipation which are unknown.

Description of turbulent reacting flows requires the understanding and prediction of situations in which the mixing is far from being complete. Another issue arising in a detailed understanding of turbulent mixing is the influence of the length scale at which the scalar fluctuations are created or injected in the flow. These considerations have led us to investigate the behaviour of a scalar field when the mixing is incomplete and in which the level of unmixedness, as well as the scalar length scale, can be controlled. We consider a simple case of homogeneous

turbulence in which both the velocity and scalar fields are statistically stationary and isotropic, using a Direct Numerical Simulation (DNS) in which both fields are randomly forced. A new technique is proposed to inject the scalar fluctuations in the simulation. This forcing technique allows us to control the scalar length scale, as well as to investigate different cases corresponding to different levels of mixing. It is presented in Section 2. Statistical isotropy and steadiness of the fields have two advantages. First, the situation is conceptually very simple and therefore is likely to be described by theoretical models. Secondly, good statistics can be obtained by averaging the results over both time and space. Furthermore, in the case of homogeneous turbulence, accurate and efficient numerical tools can be used, namely pseudo-spectral techniques. The fact that the forcing technique injects unmixed scalar fluctuations repetitively in time during the simulation disrupts the properties of the scalar field. Consequently it never develops completely and the results, although statistically stationary, have to be considered as characterizing situations which would, in the case of practical flows, correspond to the early or intermediate stages of the scalar mixing process. The results of the corresponding DNS are presented and analysed in terms of spectra and PDF in Section 3.

For real flow computations at high Reynolds number encountered in the description of practical problems, Large Eddy Simulation (LES) appears to be the most promising strategy for predicting the mixing with good accuracy. In particular, capturing the dynamics of the large eddies is important for predicting the mixing since the large scales are initiating the transfer of scalar fluctuations to the small scales. It is known that LES involves a filtering operation to remove the small scales and requires the introduction of subgrid models to restore the lost information. A key problem for applications of LES to reacting flows is to account for the scalar fluctuations at small scales and to reproduce properly the complete field statistics (and in particular the scalar PDF) which are needed to evaluate the reaction term. Among possibilities for evaluation of the PDF of the subgrid scalar fluctuations, it has been suggested [3–5] to introduce a transport equation. This equation requires closure and is generally solved by a Monte Carlo technique. The strategy adopted by Cook and Riley [1], who proposed to model the PDF using a presumed form, is simpler and was shown to lead to satisfactory results, for example in the case of a spatially growing mixing layer by Jiménez et al. [6]. In Sections 4 and 5, the results of our DNS are used to study the ability of subgrid models to reproduce the scalar PDF correctly. To this end *a priori* tests are performed, using a filter on the DNS data. The model of Cook and Riley is tested in the case of isotropic turbulence with scalar injection. In a first set of tests, the model is used with values of the subgrid-scale variance computed directly by filtering data from the DNS. A second set of tests are then performed using models for the subgrid-scale variance ("sub-models") .

Although the long term goal of the present study is the understanding and prediction of reacting and combustion flows, the problem is here addressed in the simpler case of a passive scalar in incompressible turbulence.

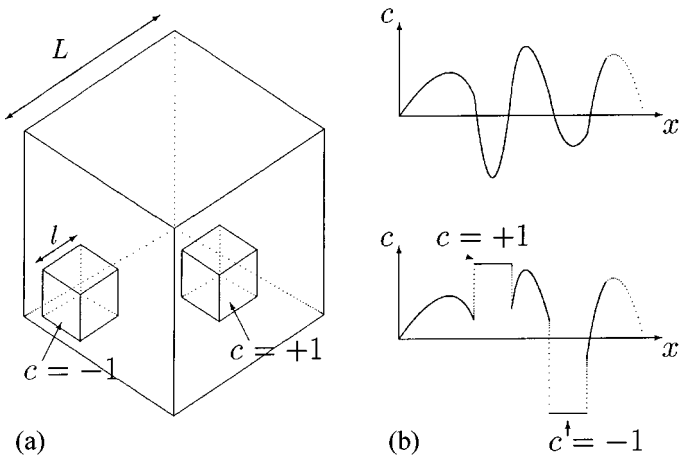

Figure 1. Illustration of the scalar injection technique in the computational domain. (a) Subboxes in which the scalar is injected ($n = 2$ in this case): $c = +1$ in one subbox and $c = -1$ in the other. (b) One dimensional scalar fluctuation along a line intersecting two subboxes, both before and after an injection.

2. Numerical Method and Injection Technique

The Navier–Stokes equation and the convection-diffusion equation for the scalar c are integrated using a pseudo-spectral method. These equations are solved in a three dimensional cubic domain of size L, with periodic boundary conditions on both the velocity and scalar. The time stepping scheme is a second-order Runge–Kutta method. The DNS are performed at a resolution of 128^3 grid points. Random Fourier mode forcing, either white-noise or time correlated (generated using a Langevin equation as proposed in [7]), is applied in the low wave-number range of the velocity spectrum. This forcing leads to a statistically steady homogeneous and isotropic velocity field.

The scalar forcing technique is illustrated by the sketch in Figure 1. It consists in "refreshing" the field by injection of unmixed fluctuations in physical space. This operation is repeated periodically in time, with a period T_i. In outline, the forcing can be summarized as follows. In the computational domain (size L), n subboxes of size l are randomly selected. In one half of these subboxes $(n/2)$, $c(x) = +1$ is imposed, whereas $c(x) = -1$ is imposed in the other half. This procedure leads to a forcing function whose PDF is essentially bi-modal. The choice of l/L allows control of the scalar integral length scale L_c and thus of the ratio $R_l = L_c/L_u$ where L_u is the velocity integral length scale. Here, L_u and L_c are defined by:

$$L_u = \frac{3\pi}{4} \frac{\int_0^\infty \frac{E_u(k)}{k}\,\mathrm{d}k}{\int_0^\infty E_u(k)\,\mathrm{d}k}, \tag{1}$$

$$L_c = \frac{\pi}{2} \frac{\int_0^\infty \frac{E_c(k)}{k}\,\mathrm{d}k}{\int_0^\infty E_c(k)\,\mathrm{d}k}, \tag{2}$$

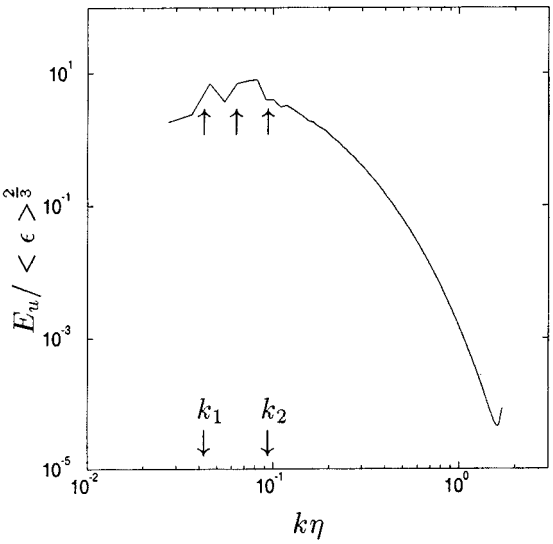

Figure 2. Turbulent kinetic energy spectrum, $E_u(K)$, at $\mathrm{Re}_\lambda = 50$ plotted using a Kolmogorov scaling; forcing was applied between k_1 and k_2 ($k_1 L = 10$, $k_2 L = 20$).

where $E_u(k)$ and $E_c(k)$ are respectively the velocity and scalar spectra. A characteristic time of injection is

$$T_{\text{res}} = T_i * \left(\frac{L^3}{n v_f} \right), \tag{3}$$

where v_f is the volume of a forced subbox. The choice of the time scale ratio

$$R_t = T_{\text{res}} / T_{\text{turb}}, \tag{4}$$

where $T_{\text{turb}} = L_u / u'$ (u' being the rms value of the fluctuation velocity) is the eddy turnover time of the turbulent field, governs the level of mixing.

In order to avoid the sharp jumps in c associated with the edges of the injection subboxes, which introduce spurious fluctuations outside the $[-1; +1]$ domain (due to Gibb's phenomenon), the injected signal is smoothed using hyperbolic tangent functions.

3. DNS Results

The simulations are performed at a Reynolds number $R_\lambda = 50$ (in which R_λ is based on the Taylor microscale (λ), $R_\lambda = u'\lambda/\nu$, ν being the viscosity) and a Schmidt number equal to 1. The spectrum of turbulent kinetic energy is plotted in Figure 2. This spectrum corresponds to the statistically steady state obtained by randomly forcing the Fourier modes between k_1 and k_2. It characterizes the velocity field that was used to obtain all results presented in the paper. Simulations

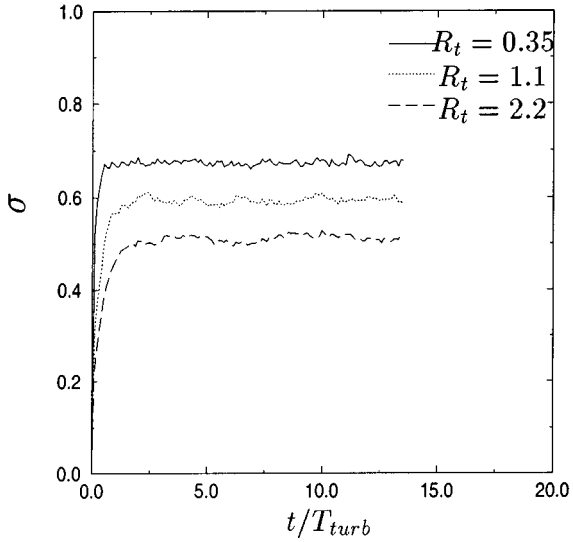

Figure 3. Time evolution of the scalar rms value for three time scale ratios, $R_t = 0.35$, $R_t = 1.1$ and $R_t = 2.2$ ($R_l = 0.71$).

were carried out using two length scale ratios ($R_l = 0.71$ and $R_l = 0.47$) and for three time scale ratios ($R_t = 2.2$, $R_t = 1.1$ and $R_t = 0.35$) expected to lead to different levels of mixing. Figure 3 shows the time evolution of the scalar rms value ($\sigma = \sqrt{\langle c^2 \rangle}$) for $R_t = 0.35$, $R_t = 1.1$ and $R_t = 2.2$ and for a given value of the length scale ratio ($R_l = 0.71$). It is seen that, after a transient period, a statistically steady state is reached. Results are time averaged once stationarity has been attained. In Figure 4, the spectrum of the scalar fluctuation corresponding to the steady state is plotted for two length scale ratios $R_l = 0.71$ and $R_l = 0.47$. It can be observed that the two spectra collapse nearly perfectly at small scales, whereas they strongly differ in the small wave-number range. The position of the maximum differs directly reflecting differences in the scales at which the scalar is injected in the flow. Although the Reynolds number is relatively low, a $K^{-5/3}$ range is apparent in the scalar spectrum for the larger length scale ratio ($R_l = 0.71$). This result is consistent with the classical analysis of Obukhov [8] and Corrsin [9] which leads to the following expression in the convective range:

$$E_c(K) = C\langle\varepsilon\rangle^{-1/3}\langle\varepsilon_c\rangle K^{-5/3}, \tag{5}$$

where $\langle\varepsilon\rangle$ is the mean dissipation rate of kinetic energy and $\langle\varepsilon_c\rangle$ is the mean dissipation rate of scalar variance. A numerical estimation of the constant C appearing in (5) gives: $C \simeq 1.1$, which corresponds to a value for the Corrsin–Obukhov constant (defined as the constant appearing in the equivalent of (5) for the one-dimensional spectrum) approximately equal to 0.65. This value is slightly larger than the ones deduced from experiments and summarized by Sreenivasan [10] (between 0.3 and 0.6). For the remainder of the paper, attention will be focused

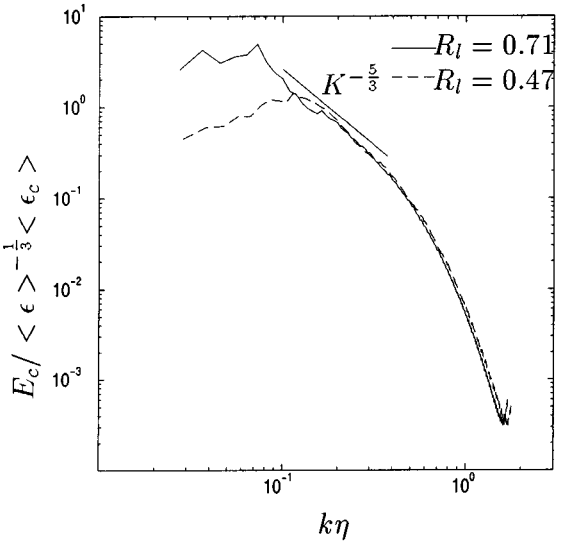

Figure 4. Scalar spectrum for two length scale ratios: $R_l = 0.71$ and $R_l = 0.47$ ($R_t = 2.2$).

on the results obtained with $R_l = 0.71$, which corresponds to the case where the spectrum is the closest to a Corrsin–Obukhov scaling.

The PDF of the scalar ($P(\Gamma) = \langle \delta(c - \Gamma) \rangle$ where $\langle \, . \, \rangle$ denotes an ensemble average and Γ denotes the value taken by the scalar fluctuation (c) were numerically estimated by generating histograms (with 60 intervals in the $[-1; 1]$ domain) and averaging over both time and space (typically one hundred 128^3 fields were used). Figure 5 shows the PDF for three time scale ratios, $R_t = 0.35$, $R_t = 1.1$ and $R_t = 2.2$. For $R_t = 0.35$, that is to say, for the value of the time scale ratio corresponding to the highest injection rate, two peaks at values of Γ close to ± 1, indicating a high level of unmixing, are clearly observed in the probability distribution. The peaks are much smaller in the case $R_t = 2.2$ corresponding to the lowest injection rate. The PDF for $R_t = 1.1$ is also given as an example of an intermediate situation. In Figure 5, it is also apparent that the shape of the PDF is affected by the injection over the whole range of fluctuations $[-1; +1]$.

Away from the two peaks, at lower injection rate, it is seen that the probability of small values of the scalar fluctuation increases, indicating that the field is more efficiently mixed. Indeed, for the lowest injection rate ($R_t = 2.2$) and small to moderate values of Γ, the PDF shows a classical Gaussian shape. This behaviour is here observed locally ($-0.5 < \Gamma < +0.5$) and sufficiently far from the two peaks associated with injection, but it indicates the presence in the field of zones where mixing is strongly affecting the scalar distribution.

It should be stressed that the PDF obtained with the present injection technique are very different from the ones obtained in the classical DNS case where the unmixed scalar is injected via the initial conditions and where the field is studied at long times (several eddy turnover times). Indeed, the present PDF show stronger

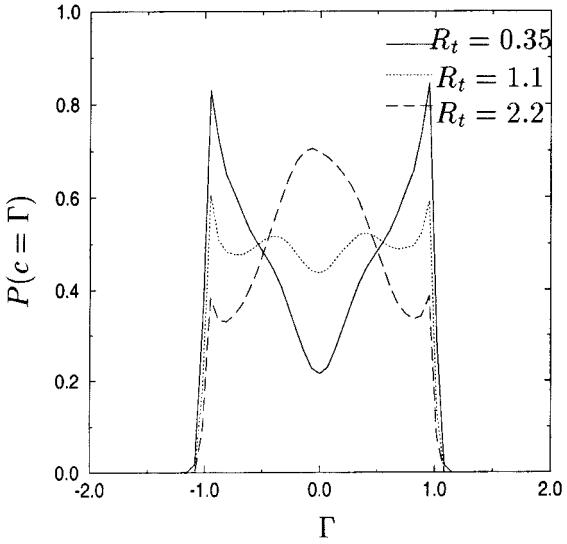

Figure 5. Probability density function of the scalar fluctuation for three time scale ratios $R_t = 0.35$, $R_t = 1.1$ and $R_t = 2.2$ ($R_l = 0.71$).

similarities with those observed in the early and intermediate stages of scalar-field development in the classical decaying case [11].

The conditional scalar dissipation ($\langle \varepsilon_c \mid c = \Gamma \rangle$) has an important effect in the PDF equation. Indeed, in the case of a decaying isotropic scalar field, it is the only unknown term appearing in the equation governing the time evolution of the PDF [2]:

$$\frac{\partial}{\partial t} P(\Gamma, t) = -\frac{\partial^2}{\partial \Gamma^2} [\langle \varepsilon_c \mid c = \Gamma \rangle P(\Gamma, t)]. \tag{6}$$

The behaviour of the conditional dissipation is analysed for different levels of mixing. In Figure 6 the conditional dissipation is plotted for the three cases corresponding to Figure 5. It may be observed that this quantity shows a strong dependency on Γ at high levels of unmixing ($R_t = 0.35$). In the case of a low injection rate ($R_t = 2.2$), this dependency tends to vanish for small and intermediate fiuctuations and the conditional dissipation nearly exhibits a plateau. This plateau is found in the range of fluctuations ($-0.5 < \Gamma < +0.5$) in which the PDF has a Gaussian shape (see Figure 5), in agreement with the classical result that Gaussianity of the scalar fluctuation is associated with uniform dissipation [12]. For the unmixed situations, the high values of the pdf near ± 1 are associated with small values of the conditional dissipation. The interpretation is that the peak values of the PDF are associated with unmixed blobs reminiscent of the injections, and that these blobs are only slightly contributing to the dissipation which mainly occurs in the rest of the domain. This interpretation is corroborated by the visualization of iso-scalar

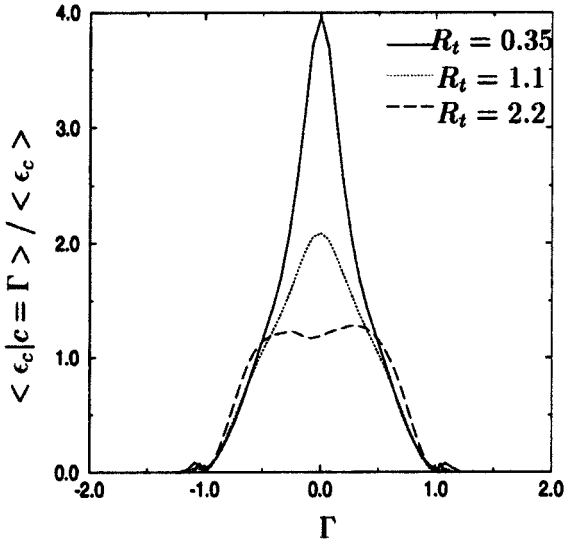

Figure 6. Normalized conditional scalar dissipation for three time scale ratios $R_t = 0.35$, $R_t = 1.1$ and $R_t = 2.2$ ($R_l = 0.71$).

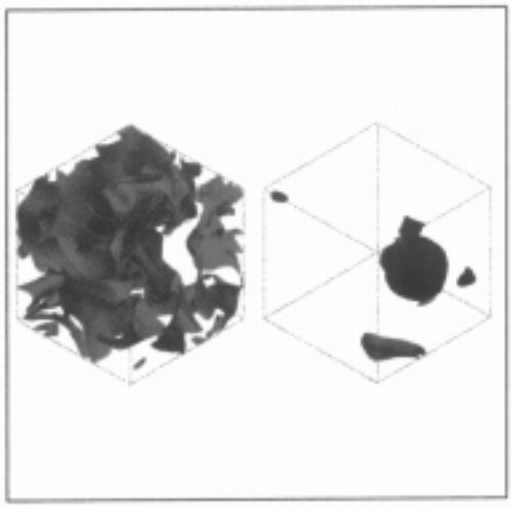

Figure 7. Visualization of the iso-scalar contours; $c = \pm 0.9$ on the right and $c = 0$ on the left. Each box corresponds to one-eighth of the computational domain.

contours presented in Figure 7, where the blobs can be seen for $c = \pm 0.9$, whereas in the rest of the domain, small scales fluctuations are observed ($c = 0$).

4. Application to LES and Subgrid Modeling

In LES only the large scales are computed. They are separated from the rest of the field by applying a filter G. The large scale component $\bar{c}$ of the scalar fluctuation c is thus:

$$\bar{c}(\mathbf{x}, t) = \iiint_V G(|\mathbf{x} - \mathbf{x}'|)c(\mathbf{x}', t)\, \mathrm{d}\mathbf{x}' \tag{7}$$

and the subgrid fluctuation is

$$c' = c - \bar{c}. \tag{8}$$

The equation for the filtered scalar field reads:

$$\frac{\partial \bar{c}}{\partial t} + \bar{u}_i \frac{\partial \bar{c}}{\partial x_i} = D\frac{\partial^2 \bar{c}}{\partial x_i^2} - \frac{\partial \tau_i}{\partial x_i} - \frac{\partial \mathcal{L}_i}{\partial x_i} \tag{9}$$

in which τ_i and $\mathcal{L}_i$ are respectively the subgrid and Leonard contributions:

$$\begin{aligned} \tau_i &= \overline{u_i'\bar{c}} + \overline{\bar{u}_i c'} + \overline{u_i' c'}, \\ \mathcal{L}_i &= \overline{\bar{u}_i \bar{c}} - \bar{u}_i \bar{c}. \end{aligned} \tag{10}$$

The key problem for applications of LES to reacting flows is whether the subgrid models used to account for the small scales can properly reproduce the statistics of the whole field. The problem is twofold, the first question being whether the effect of the unresolvable scales on the dynamics of large scales can be correctly taken into account. This is the classical question of modeling the τ_i subgrid term appearing in (9) (and its counterpart in the equation for the velocity), by introducing a model usually based on the concept of eddy diffusivity (respectively eddy viscosity in the $\bar{u}$ equation). The second question is more specifically related to reacting flows. It is whether the contribution of the small scales, c', to the scalar statistics can be satisfactorily modeled.

In the present paper, we almost exclusively address the second question; the influence of the modeling of τ_i being only very briefly discussed at the end of Section 6. The question is addressed using the DNS results presented in the previous section as a data base to perform *a priori* tests of the Cook and Riley [1] subgrid model. The filter for these tests is a top hat filter of width h in physical space.

In LES of a reacting flow, one is primarily interested in predicting the filtered reaction rate $\bar{w}$ at every point. Since w is generally a highly nonlinear function of the scalar fluctuation (c being for example identified with the mixture fraction z in this case) what is needed is not only information on the low order moments of the scalar fluctuation, but details of its statistical distribution. In the case of the equilibrium chemistry limit, the filtered reaction rate $\bar{w}$ can be expressed as a function of the PDF of the scalar fluctuations inside the filter volume (or "subgrid PDF")

$$P_h(c; \bar{c}), \tag{11}$$

a quantity which clearly depends on the scalar distribution at small scales (smaller than the filter width h).

The above PDF is precisely the quantity that Cook and Riley [1] proposed to model using β functions. This assumed PDF approximation leads to a family of PDF which can be used to interpolate smoothly between different cases of mixing taking into account the constraint that the fluctuation is confined to a bounded interval. This type of approach is often used to evaluate the distribution of the complete scalar field in Reynolds averaged calculations [13]. Following Cook and Riley [1], the β distribution is here used to approximate the scalar PDF at small scales (see also [6, 14]). For a scalar varying between -1 and $+1$, the β distribution has the form:

$$P_h(c;\bar{c},c_s) = \frac{\left(\frac{1+c}{2}\right)^{a-1}\left(\frac{1-c}{2}\right)^{b-1}}{2B(a,b)} \tag{12}$$

in which a and b can be expressed in terms of the filtered scalar $\bar{c}$ and subgrid variance c_s^2.

$$a = \left(\frac{1+\bar{c}}{2}\right)\left(\frac{(1+\bar{c})(1-\bar{c})}{c_s^2} - 1\right), \tag{13}$$

$$b = \frac{1-\bar{c}}{1+\bar{c}}\,a, \tag{14}$$

$$c_s^2 = \overline{c^2} - \bar{c}^2. \tag{15}$$

As pointed out by Cook and Riley [1], once P_h is specified, the complete scalar PDF can be reconstructed. In the case of homogeneous turbulence this can be done using the relation:

$$P(c) = \iint P_c(\bar{c},c_s)\,P_h(c;\bar{c},c_s)\,\mathrm{d}\bar{c}\,\mathrm{d}c_s, \tag{16}$$

where P_c, is the joint probability of the filtered scalar and of the subgrid rms value.

In the next section, use will be made of our DNS data base to evaluate the Cook and Riley subgrid model as a satisfactory assumption of the small scale statistics. The criteria for these tests will be the ability of the model to reproduce the PDF of the whole scalar field $P(c)$ knowing the filtered field $\bar{c}$. Such a criteria is of importance because $P(c)$ directly governs the mean reaction rate. A satisfactory reproduction of $P(c)$ by the model also gives an indication that the subgrid PDF P_h is correctly modeled and hence that the model is likely to be trustworthy when used to predict the local reaction rate $\bar{w}$ for LES of complex reacting flows. For a real LES computation, the subgrid variance appearing in (12), c_s^2, needs to be estimated (introducing what is referred to as a "submodel"). However, in the next section c_s^2 is directly deduced from the DNS using (15). In Section 6, the influence of using a submodel for c_s^2 will be investigated.

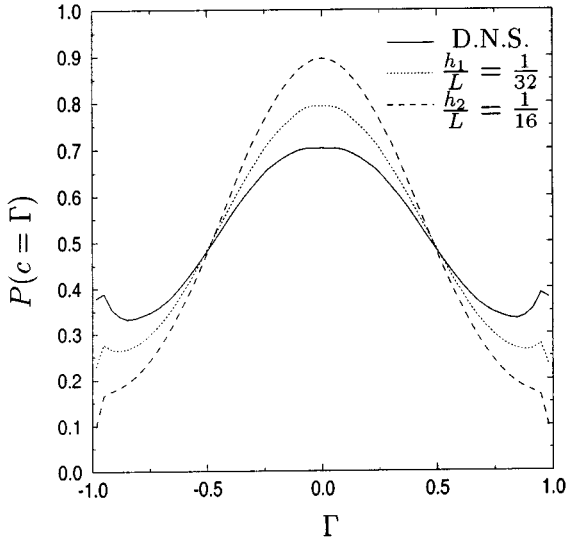

Figure 8. Probability density function of the scalar for filtered ($h_1/L = 1/32$ and $h_2/L = 1/16$) and unfiltered DNS results; $R_t = 2.2$, $R_l = 0.71$.

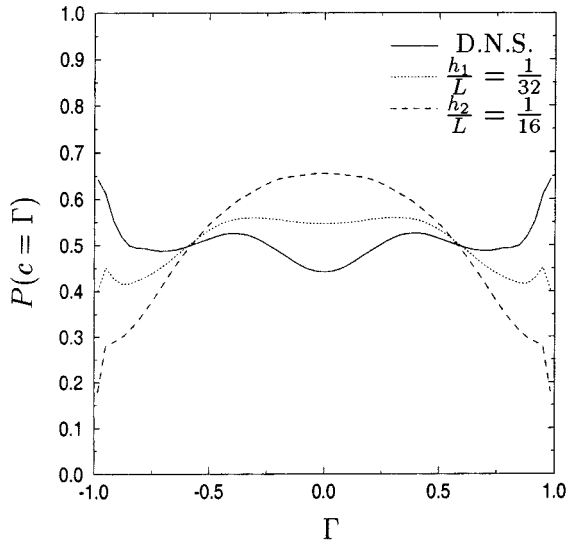

Figure 9. Same as Figure 8, but with $R_t = 1.1$.

5. Filtered Results and Reconstructed Scalar PDF

To investigate the effect of the filtering operation in a LES, the filter was applied to the DNS results presented in Section 3. Two filter widths h_1 and h_2 ($h_1/L = 1/32$, $h_2/L = 1/16$) were used. The scalar PDF for the filtered and unfiltered results are compared in Figures 8–10, for three time scale ratios. It can be observed that,

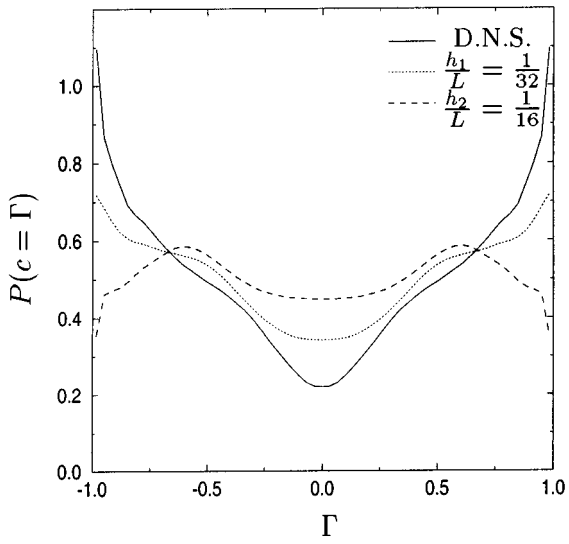

Figure 10. Same as Figure 8, but with $R_t = 0.35$.

compared to the unfiltered field, the PDF of the filtered scalar exhibits smaller peaks at $c = \pm 1$ and a higher value at small fluctuations. It can also be observed that the influence of the filtering is more important for larger filter width. These results are in agreement with those of Jiménez et al. [6]. It should be mentioned that the DNS results plotted in Figures 8–10 were slightly corrected before applying the filter: spurious fluctuations larger than 1 (or smaller than -1) were assigned to be equal to 1 (respectively -1). This correction was introduced in order to avoid working with values of $\bar{c}$ outside the $[-1 : 1]$ domain in the study presented below.

The filtered scalar was used to test the reconstruction technique proposed by Cook and Riley [1] and described above. The test was performed for the three cases of mixing and for the two filter widths. The reconstructed PDF were compared with the complete PDF in Figures 11–13 for $R_t = 2.2$, $R_t = 1.1$ and $R_t = 0.35$ respectively. It is seen that there is good agreement between the reconstructed and complete PDF. The reconstruction is less accurate at high injection rates, when there is a high level of unmixing, whereas for the lowest injection rate ($R_t = 2.2$) the agreement is nearly perfect, except near $+1$ and -1. It has to be pointed out that the discrepancies observed between the DNS and recontructed PDF near $+1$ and -1 should not necessarily be interpreted as a deficiency of the subgrid model. They could also be partially attributed to an imperfection in the DNS data base: in the DNS, the peaks are not exactly situated at $+1$ and -1 as appears in Figure 11. In Figures 11–13 it is also observed that, as expected, the PDF is reconstructed with more accuracy for the smaller filter width.

The above results were obtained using (15) to estimate locally the subgrid variance directly from the DNS data. Before investigating the problem of modeling the subgrid variance, we first checked the importance of a local estimation of c_s^2. We

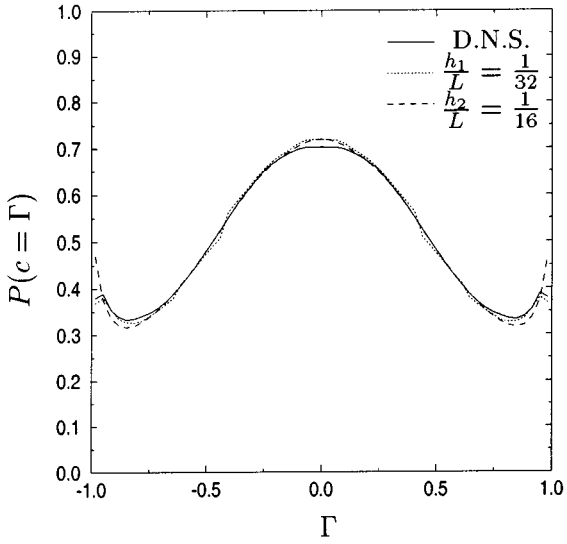

Figure 11. Reconstructed and unfiltered probability density functions; $R_t = 2.2$. Results obtained with exact subgrid variance.

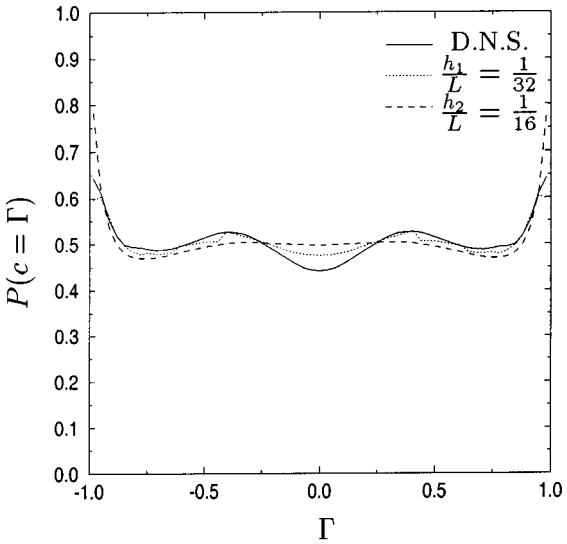

Figure 12. Same as Figure 11, but with $R_t = 1.1$.

performed a test using an averaged estimation of c_s^2 ($\langle c_s^2 \rangle_D$ in which $\langle \, . \, \rangle_D$ denotes the average over the computational domain) in P_h, instead of the local values. In Figure 14 it is seen that the agreement with the DNS is less satisfactory with the averaged estimation of c_s^2 than with the local one. This is particularly true at large fluctuations, where the averaged estimation leads to a strong overprediction of the PDF.

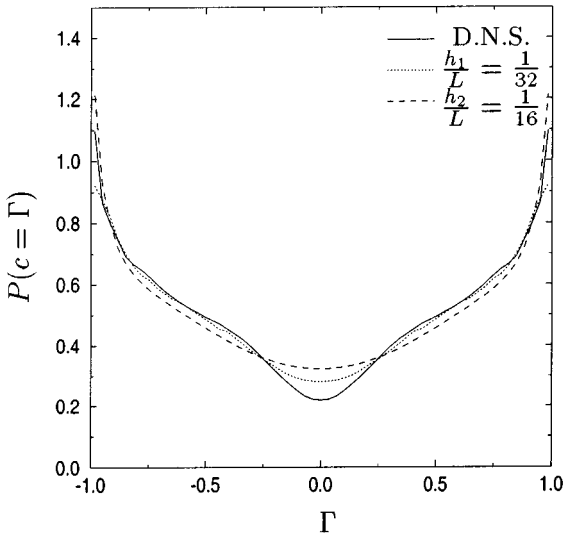

Figure 13. Same as Figure 11, but with $R_t = 0.35$.

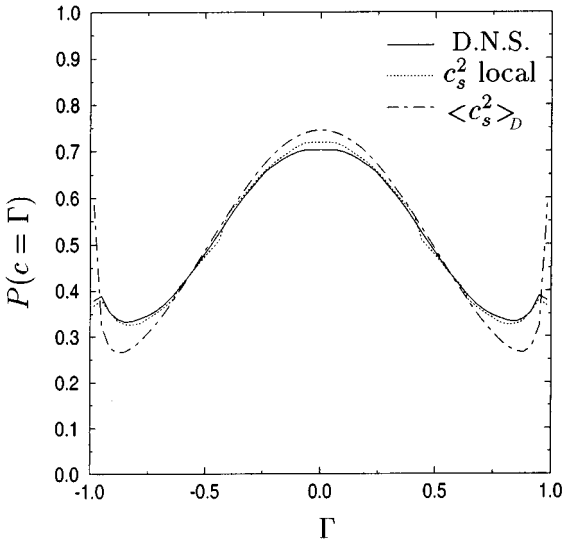

Figure 14. Reconstructed probability density functions. Comparison between results obtained with local and averaged c_s^2 ($h_1/L = 1/32$, $R_t = 2.2$).

6. Influence of the Submodel for the Subgrid Variance

As stated above, before using the presumed PDF distribution, in a real LES the scalar subgrid variance has to be estimated, and it is important to reproduce correctly the local variations of this quantity. It has been suggested [1] to follow

the idea of scale similarity proposed by Ferziger [16] and hence to estimate c_s^2 introducing a double filtering procedure

$$c_s^2 = C_s\left(\widehat{\bar{c}^2} - \widehat{\bar{c}}^2\right) \tag{17}$$

in which $\widehat{(.)}$ denotes a filter with a larger width than the filter $\overline{(.)}$ and in which C_s is a constant. This constant has to be evaluated. C_s can be interpreted as the ratio between the variances of scalar fluctuations contained in two different parts of the spectrum: the variance in the subgrid part of E_c and the variance in the intermediate range between the test and true filters. C_s can then be evaluated by spectral integration, once the spectrum E_c and the filter characteristics are specified, as suggested by Cook [17]. Assuming a $K^{-5/3}$ spectrum for the scalar fluctuation and an infinite Reynolds number, Jiménez et al. [6] found $C_s = 1.7$. Cook and Riley [1] found $C_s = 0.81$ by computing its value from their DNS. Réveillon and Vervisch [14] (see also [6]) used $C_s = 0.25$.

An alternative route is to follow Sarkar et al. [18] who recently proposed to use a Taylor expansion technique for modeling the subgrid moments of the scalar fluctuations. This technique can be used to estimate C_s. Instead of using (17), the subgrid variance is expressed as:

$$c_s^2 = C_s\left(\overline{\bar{c}^2} - \bar{\bar{c}}^2\right). \tag{18}$$

It should be noted that (17) and (18) are based on the same scale similarity assumptions, the effect of applying the same filter twice being of the same nature as applying a larger width filter. Only the numerical value for C_s is modified.

Then a Taylor expansion of Equations (18) and (15) is performed. This procedure leads to express C_s as [19]:

$$C_s \simeq \frac{\bar{c}}{\bar{\bar{c}}}\,\frac{\Delta\bar{c}}{\Delta\bar{\bar{c}}}. \tag{19}$$

It is important to stress that in this case C_s is locally estimated, whereas in the classical approach it is a constant that depends only on the statistically averaged scalar spectrum (and on the filter characteristics).

Figures 15–17 show comparisons between the unfiltered DNS PDF and the reconstructed PDF, for two filter widths $h_1/L = 1/32$ and $h_2/L = 1/16$, for $R_t = 2.2$, $R_t = 1.1$ and $R_t = 0.35$, with the subgrid variance expressed by (18) and with the local estimation (19) of C_s. It is seen that good agreement between the reconstructed and the unfiltered PDF is found for all three cases, the detailed shape of the PDF being better reproduced for the well mixed situation ($R_t = 2.2$). When compared to the results presented in the previous section (where the subgrid variance was directly computed from the DNS), it appears that the results are now less accurate but that the agreement still remains satisfactory.

In order to study the influence of the local estimation of C_s, we present results obtained with the classical formulation (Equation (17) with C_s constant). In this

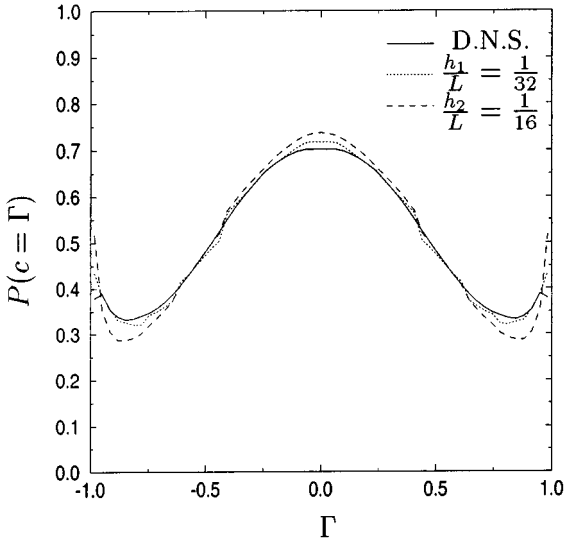

Figure 15. Reconstructed and unfiltered probability density functions ($R_t = 2.2$). Results obtained using scale similarity estimation of the subgrid variance and local estimation of the constant in (18); $h_1/L = 1/32$, $h_2/L = 1/16$.

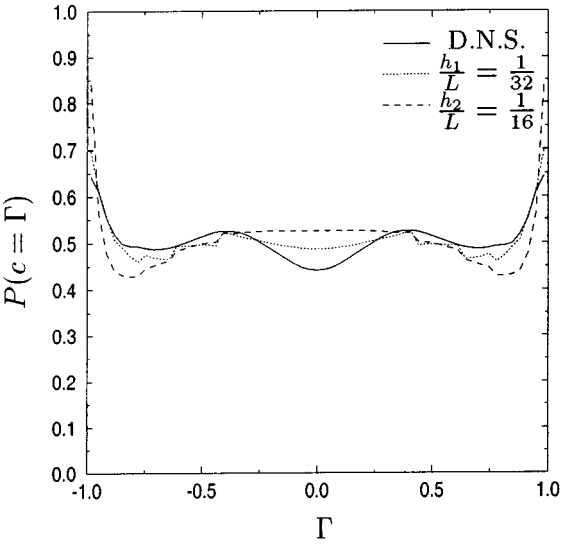

Figure 16. Same as Figure 15, but with $R_t = 1.1$.

case the test filter is a top hat filter whose width is twice the true filter width. Figure 18 shows the reconstructed PDF obtained with three values for C_s ($C_s = 0.25$, $C_s = 0.81$ and $C_s = 1.7$ respectively corresponding to the values used in [1, 6, 14]). The results obtained with the classical formulation (C_s constant), although remaining acceptable, show larger errors than the ones obtained using

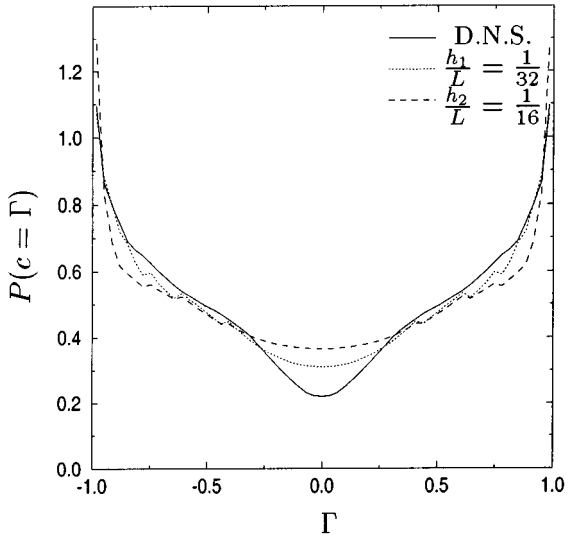

Figure 17. Same as Figure 15, but with $R_t = 0.35$.

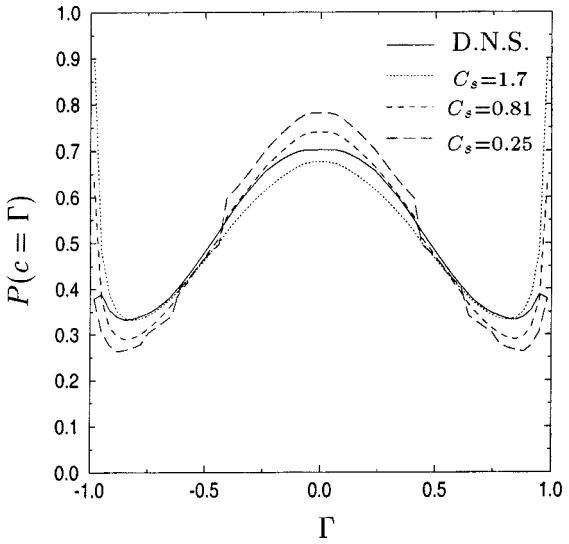

Figure 18. Reconstructed and unfiltered probability density functions ($R_t = 2.2$). Results obtained using the Cook and Riley model for the subgrid variance for $C_s = 0.25$, $C_s = 0.81$ and $C_s = 1.7$; $h_1/L = 1/32$.

(18) and (19) (Figure 15, $h_1/L = 1/32$). It may be concluded that a significant improvement of the reconstruction of the PDF is obtained when local estimation of C_s is performed using the technique proposed in [18].

As mentioned above, another source of error in LES is the effect of the subgrid model on the resolved scalar field itself, that is to say, the effect of the modeling of

τ_i via an eddy diffusivity to account for the cascade process in the scalar spectrum. Although we did not perform a detailed study of this effect, preliminary results of *a posteriori* tests [20] show that, when compared to the error associated with the subgrid scalar fluctuation (using the Cook and Riley model [1]), the errors resulting from the use of an eddy diffusivity appear to be of the same order or larger.

7. Conclusions

DNS of isotropic turbulence were performed with an injection technique for scalar fiuctuations leading to statistically steady states associated with different levels of mixing. The scalar PDF and its conditional dissipation were found to strongly depend on the level of mixing. At high injection rates, the PDF is nearly bi-modal with two peaks corresponding to blobs of nearly uniform concentration $c \simeq \pm 1$ reminiscent of the injections. At low injection rates, although the peaks are still present, they are much smaller and there is an intermediate range of fluctuations in which the PDF is nearly Gaussian refiecting the existence of a plateau of uniform conditional dissipation.

The PDF show strong similarities with those observed in the early and intermediate stages of the development of the scalar field in studies where the unmixed scalar is injected via the initial condition. The present injection technique allows one to obtain these types of PDF in statistically steady situations, which has the advantage of permitting time averaged statistics.

The properties of the scalar fields generated by the injection technique are perhaps somewhat artificial. A question that can then be raised is the physical relevance of such fields. On the one hand, the injection technique may be considered as a numerical tool, some of the properties of the resulting fields then possibly being artifacts. On the other hand, it is possible to imagine experimental situations sharing strong similarities with the one numerically studied in this paper. It has for example been proposed to inject temperature fluctuations in water by micro-waves [21].

Using the DNS results to perform *a priori* tests of subgrid models has shown that the error induced in the PDF by the filtering operation can be efficiently corrected using the presumed PDF subgrid model of Cook and Riley [1]. Such a conclusion is in agreement with several previous studies, and in particular that of Jiménez et al. [6] in the case of a temporally growing mixing layer.

Results obtained using a direct estimation of the scalar subgrid variance from the DNS data lead to very good agreement with the unfiltered DNS data.

Special attention has been devoted to the effect of the submodels used to estimate the subgrid variance in the Cook and Riley model. It was found that models based on scale similarity arguments for the subgrid variance gave satisfactory results, especially when a local estimation of the model constant was performed.

References

1. Cook, A.W. and Riley, J.J., A subgrid model for equilibrium chemistry in turbulent flows. *Phys. Fluids* **6** (1994) 2868–2870.
2. Libby, P.A. and Williams, F.A. (eds), *Turbulent Reacting Flows*. Academic Press, New York (1980).
3. Gao, F. and O'Brien, E.E., A large eddy scheme for turbulent reacting flows. *Phys. Fluids A* **5**(6) (1993) 1282–1284.
4. Colucci, P.J., Jaberi, F.A., Givi, P. and Pope, S.B., Filtered density function for large eddy simulation of turbulent reacting flows. *Phys. Fluids* **10**(2) (1998) 499–515.
5. Réveillon, J. and Vervisch, L., Subgrid-scale turbulent micromixing: Dynamic approach. *AIAA J.* **36**(3) (1998) 336–341.
6. Jiménez, J., Linán, A., Rogers, M.M. and Higuera, F.J., A priori testing of subgrid models for chemically reacting non-premixed turbulent shear flows. *J. Fluid Mech.* **349** (1997) 149–171.
7. Eswaran, V. and Pope, S.B., An examination of forcing in Direct Numerical Simulation of turbulence. *Comput. & Fluids* **16**(3) (1988) 257–278.
8. Obukhov, A.M., Structure of the temperature field in tubulent flow. *Izv. AN SSSR, Ser. geogr. i geofiz.* **38**(13) (1949) 58–69.
9. Corrsin, S., On the spectrum of isotropic temperature fluctuations in an isotropic turbulence. *J. Appl. Phys.* **22**(4) (1951) 469–473.
10. Sreenivasan, K.R., The passive scalar spectrum and the Obukhov–Corrsin constant. *Phys. Fluids* **8**(1) (1996) 189–196.
11. Eswaran, V. and Pope, S.B., Direct numerical simulations of the turbulent mixing of a passive scalar. *Phys. Fluids* **31**(3) (1988) 506–520.
12. O'Brien, E.E. and Jiang, T.L., The conditional dissipation rate of an initially binary scalar in homogeneous turbulence. *Phys. Fluids A* **3**(12) (1991) 3121–3123.
13. Miller, R.S., Frankel, S.H., Madnia, C.K. and Givi, P., Johnson–Edgeworth translation for probability modeling of binary scalar mixing in turbulent flows. *Combust. Sci. Technol.* **91** (1993) 21–52.
14. Réveillon, J. and Vervisch, L., Response of the dynamic LES model to heat release induced effects. *Phys. Fluids* **8** (1996) 2248–2250.
15. Chollet, J.P. and Lesieur, M., Parameterization of small scales of three-dimensional isotropic turbulence utilizing spectral closures. *J. Atmos. Sci.* **38** (1981) 2747–2757.
16. Ferziger, J.H., Higher-level simulations of turbulent flows. In: Essers, J.A. (ed.), *Computational Methods for Turbulent, Transonic, and Viscous Flows*. Hemisphere, New York (1983) p. 93.
17. Cook, A.W., Determination of the constant coefficient in scale similarity models of turbulence. *Phys. Fluids* **9**(5) (1997) 1485–1487.
18. Sarkar, S., Shao, L. and Pantano, C., A subgrid scale model for scalar moments encountered in turbulent combustion. APS Meeting, New Orleans (1999).
19. Shao, L., Private communication.
20. Elmo, M., Bertoglio, J.P. and Sabel'nikov, V.A., Mixing in isotropic turbulence with scalar injection and applications to subgrid modeling. In: Banerjee, S. and Eaton, J.K. (eds), *Turbulence and Shear Flow Phenomena*. Santa Barbara, Begellhouse (1999) pp. 869–874.
21. Plaza, F., Private communication.